Photonic crystal slab cavity simultaneously optimized for ultra-high Q/V and vertical radiation coupling

Momchil Minkov, Vincenzo Savona, and Dario Gerace

Citation: Appl. Phys. Lett. **111**, 131104 (2017); doi: 10.1063/1.4991416
View online: http://dx.doi.org/10.1063/1.4991416
View Table of Contents: http://aip.scitation.org/toc/apl/111/13
Published by the American Institute of Physics

Articles you may be interested in

Q factor limitation at short wavelength (around 300 nm) in III-nitride-on-silicon photonic crystal cavities
Applied Physics Letters **111**, 131103 (2017); 10.1063/1.4997124

Polarization-entangled photons from an InGaAs-based quantum dot emitting in the telecom C-band
Applied Physics Letters **111**, 133106 (2017); 10.1063/1.4994145

Clocking plasmon nanofocusing by THz near-field streaking
Applied Physics Letters **111**, 131102 (2017); 10.1063/1.4991860

Radiation-induced direct bandgap transition in few-layer MoS_2
Applied Physics Letters **111**, 131101 (2017); 10.1063/1.5005121

Nonlinear terahertz metamaterials with active electrical control
Applied Physics Letters **111**, 121101 (2017); 10.1063/1.4990671

Experimental demonstration of Fabry-Perot open resonators in a surface-wave bandgap crystal
Applied Physics Letters **111**, 121102 (2017); 10.1063/1.4993300

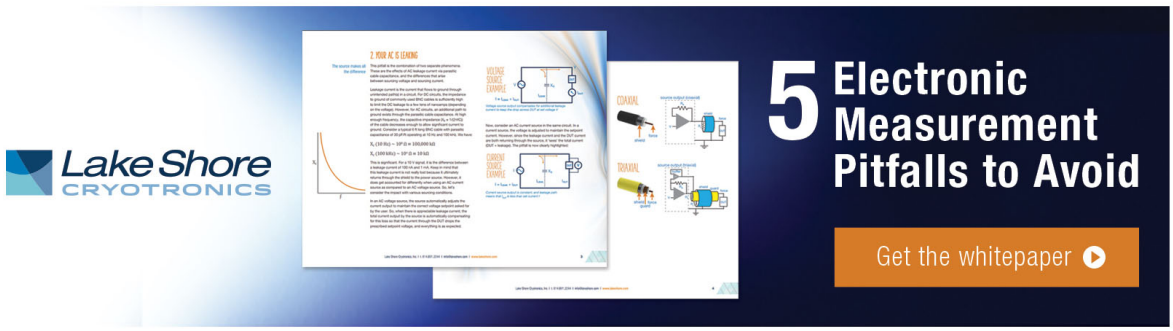

Photonic crystal slab cavity simultaneously optimized for ultra-high *Q*/*V* and vertical radiation coupling

Momchil Minkov,[1,a)] Vincenzo Savona,[2] and Dario Gerace[3]
[1]*Department of Electrical Engineering, and Ginzton Laboratory, Stanford University, Stanford, California 94305, USA*
[2]*Institute of Theoretical Physics, Ecole Polytechnique Fédérale de Lausanne EPFL, CH-1015 Lausanne, Switzerland*
[3]*Department of Physics, University of Pavia, Via Bassi 6, 27100 Pavia, Italy*

(Received 20 June 2017; accepted 13 September 2017; published online 28 September 2017)

We present a design for a two-dimensional photonic crystal slab cavity in which the electric field localization is due to an extra hole in the lattice, as opposed to the more standard procedure of removal of holes. This leads to a tighter field confinement and a mode volume that is several times smaller than that of conventionally used designs. Through small modifications of the holes around the cavity, we optimize the theoretical quality factor (Q) to an ultra-high value of 20.9×10^6 and furthermore illustrate the possibility for high coupling efficiency to free-space modes in the vertical direction, while keeping a high Q of 3.7×10^6. *Published by AIP Publishing.*
[http://dx.doi.org/10.1063/1.4991416]

Current research in photonics is heavily directed towards on-chip integration and interfacing with electronic components for faster and more efficient information transmission and processing.[1] Photonic crystals (PhCs) hold great promise to advance this effort due to their natural silicon-chip integrability and their ability to tightly confine light with minimal losses to the environment.[2] A PhC optical cavity[3–10] in particular provides the strongest known all-dielectric concentration of light to volumes of the order of a cubic wavelength, together with a photon lifetime with a characteristic quality factor (Q) that can exceed one million. This cavity has thus become a fundamental building block for various applications in the domains of classical and quantum communications, lasers, and sensing.[11–28] There are a number of different PhC cavities, but one of the most widely used is the *L*3 design, formed by three missing holes in a hexagonal lattice of air-holes in a dielectric slab.[3,10–14,21–25] In this Letter, we present a different way to introduce a localized mode in the slab-PhC lattice, namely, by *adding* instead of removing holes, which results in a stronger field confinement. Furthermore, we optimize the theoretical quality factor of the proposed device to 20.9×10^6 and thus obtain a structure superior to the traditional *L*3 in all respects, without any added disadvantages.

Broadly speaking, resonators are used to enhance light-matter interactions such as material non-linearities or coupling to emitters. While the exact description of these interactions varies, they are all enhanced by a stronger concentration of electromagnetic energy, and so, the quality factor of a cavity is a fundamental figure of merit. It is worth noting, however, that in experiments, this quantity does not always match the *intrinsic* (theoretical) value predicted by simulations but is instead limited by structural disorder and/or absorption.[29,30] Thus, while intrinsic Q values above one billion have been predicted,[7,8] the record measured Q was recently reported to be eleven million[9] and values above one million are considered ultra-high. Thus, merely improving the intrinsic Q of a cavity is not always associated with an improvement in practice, in particular when the theoretical value is of the order of tens of millions. Thus, another important cavity figure of merit is the modal volume, which can be defined for example as

$$V_m = \frac{\int_V |\mathbf{E}_m(\mathbf{r})|^2 \varepsilon(\mathbf{r}) d\mathbf{r}}{\max_{\mathbf{r}} \left[|\mathbf{E}_m(\mathbf{r})|^2 \varepsilon(\mathbf{r}) \right]}, \tag{1}$$

where $\mathbf{E}_m(\mathbf{r})$ is the electric field profile of the mode, $\varepsilon(\mathbf{r})$ is the dielectric permittivity, and the integration is over the whole space. This definition of the volume, particularly relevant for light coupling to point-like emitters, is now commonly adopted in the PhC literature. We will thus use it throughout this Letter, but we note that other definitions are possible and reasonable for other applications.[31] These all scale down with the confinement of the electric field to physically smaller structures, and the smallest possible volumes are usually desired.

The standard *L*3 cavity is illustrated in Fig. 1(a). We assume a silicon (Si) slab of thickness $d = 220$ nm and a hexagonal lattice of air-holes of radius $r = 100$ nm, with a lattice period of $a = 420$ nm. The lowest-frequency localized mode is found at $\lambda = 1.604\ \mu$m and has a quality factor of $Q = 7200$, and the mode volume is $V_m = 0.64(\lambda/n)^3$, computed using a 3D finite-difference time-domain (FDTD) commercial solver.[32] This basic design has a modest quality factor, but it has been shown that small modifications of the holes surrounding the cavity can lead to a tremendous increase in Q,[33,34] combined with a much less significant increase in the mode volume. Notably, a design with a theoretical $Q = 4.1 \times 10^6$ and a mode volume of $V_m = 0.95(\lambda/n)^3$ has been proposed and experimentally characterized.[10,34]

In Fig. 1(b), we illustrate our cavity proposal, which is based on the same slab-PhC, but with one *additional* hole in the lattice. The design is even better understood as four holes

a)mminkov@stanford.edu

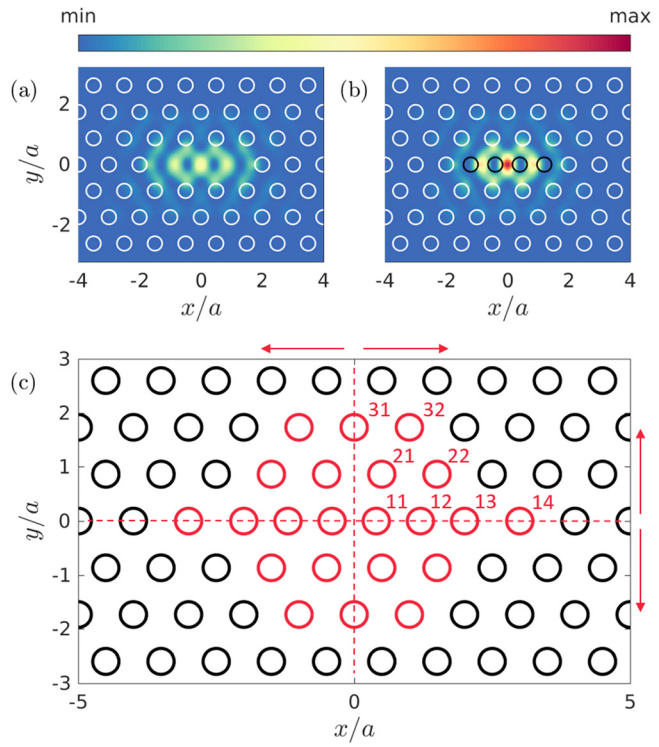

FIG. 1. (a) Electric field $|\mathbf{E}|^2$ profile in the center of the slab for an $L3$ cavity. (b) The same as (a), for the $L4/3$ design. The four additional holes are marked in black. (c) The positions of the holes marked in red are shifted for quality factor optimization of the $L4/3$ cavity. The shifts are symmetrical with respect to the center, where the two dashed lines intersect. The modified holes are labeled by two digits given by their row and column number, respectively.

(marked in black) added in the region where the three holes of the $L3$ cavity are removed. Because of this, we refer to it below as the $L4/3$ cavity. The electric field of its fundamental mode is also illustrated in the Figure. The fields shown in Figs. 1(a) and 1(b) are normalized so that $\int_V |\mathbf{E}(\mathbf{r})|^2 \varepsilon(\mathbf{r}) d\mathbf{r} = 1$ and are plotted on the same color scale. This perfectly illustrates the effect of the four extra holes: the mode profile of the $L4/3$ cavity is reminiscent of that of the $L3$, but the field is squeezed more tightly in the cavity center. Indeed, the mode volume for the structure of panel (b) is found to be $V_m = 0.35(\lambda/n)^3$, and the quality factor is $Q = 33\,000$. Because of the tighter confinement, the mode also lies at a lower resonance wavelength, $\lambda = 1.547\ \mu$m.

Next, we optimize Q of this $L4/3$ cavity using an approach similar to that in Ref. 34. More precisely, we vary the positions of the holes closest to the center of the cavity and use a global optimization algorithm[35] (specifically, particle-swarm optimization) to find the maximum Q with respect to these structural parameters. For an efficient and reliable computation of each structure, we perform a simulation using the guided-mode expansion method.[34,36] Once an optimal structure is obtained, a first-principles FDTD simulation[32] is also performed, to verify all the parameters of the cavity mode. As optimization parameters, we include the positions of all holes marked in red in Fig. 1(c). We denote the shifts along the x- and y-axes as X_{ij} and Y_{ij}, respectively, where the indexes ij for each hole are marked in the Figure. We apply the shifts symmetrically with respect to both the xz and yz planes [red dotted lines in Fig. 1(c)], i.e., the values of X_{ij} and Y_{ij} need to be set only for the holes in one of the four quadrants. Furthermore, we define the positive direction of the shifts to be away from the center of the cavity [cf. red arrows in Fig. 1(c)]. Finally, we note that the symmetry also imposes, for all i, j, $Y_{1j} = 0$, and $X_{i1} = 0$. Thus, in total, there are eleven optimization parameters for the holes marked in red in Fig. 1(c).

Using the quality factor as an objective function, the optimal design is found for $X_{1,1-4} = [-0.013, -0.018, 0.044, 0.200]a; X_{2,1-2} = [0.052, 0.065]a; X_{32} = -0.005a; Y_{2,1-2} = [0.101, 0.044]a; Y_{3,1-2} = [-0.013, -0.032]a$. We note once more that negative values signify shifts in the direction opposite to the red arrows in Fig. 1(c). The electric field of the optimized cavity mode and the optimized hole positions are illustrated in Fig. 2. The design has a theoretical, FDTD-computed Q of 20.9×10^6. Furthermore, unlike previous quality-factor optimizations,[34] the mode volume actually *decreases* slightly, compared to the un-optimized design, and was found to be $V_m = 0.32(\lambda/n)^3$. This is likely related to the fact that the shift X_{11} is negative, bringing the two holes closer to the center of the cavity.

The figures of merit of our optimized cavity are compared in Table I against the most relevant existing designs. Compared to the $L3$ cavity in Ref. 34, the mode volume of $L4/3$ is three times smaller, while the theoretical Q is five times larger. The only known designs with a higher theoretical Q are the various waveguide-based cavities,[5–9] for which this parameter can go up to one billion.[7,8] However, as discussed earlier and shown in the last two columns of the Table, the measured Q is limited by disorder (and potentially material losses) such that statistically similar values can be expected for any cavity design with a theoretical Q larger than about ten million.[9,29,30] The comparison in the Table shows that there is a rough, negative correlation between the mode volume and the disorder-averaged Q-values, which can be understood intuitively since the same change in the

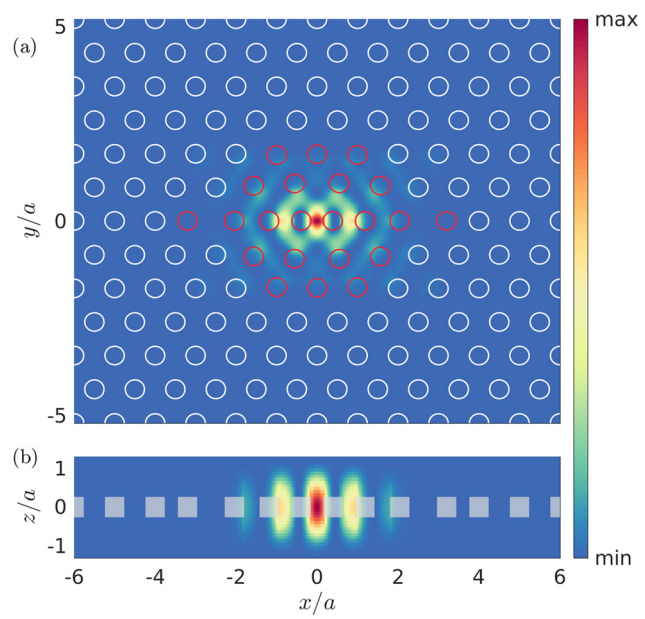

FIG. 2. Electric field $|\mathbf{E}|^2$ profile for the optimized cavity mode: (a) in the x-y plane, for $z = 0$ and (b) in the x-z plane, for $y = 0$. The holes whose positions were changed are marked in red in (a).

TABLE I. Comparison of the cavity design proposed here with other relevant slab-PhC cavities. All Q values are in millions, and $\langle Q\rangle$ denotes the average simulated Q assuming Gaussian disorder in the positioning and radius of the holes with zero mean and standard deviation $\sigma_1 = 1.2$ nm or $\sigma_2 = 0.6$ nm. One hundred disorder realizations were computed for *L*4/3.

Cavity	$V_m\,(\lambda/n)^3$	Q	$\langle Q\rangle_{\sigma_1}$	$\langle Q\rangle_{\sigma_2}$
*L*4/3 (this work)	0.32	20.9	1.8	0.55
Optimized *L*3 (Ref. 34)	0.95	4.1	2.5	0.93
Waveguide-based[5–9]	$\gtrsim 1.2$	>50	2.9[a]	0.86[a]
Optimized *H*0 (Ref. 34), v. 1	0.25	1.0	0.7	0.40
Optimized *H*0 (Ref. 34), v. 2	0.64	8.9	2.0	0.65

[a]Values extrapolated from Ref. 29 for the cavity in Ref. 5.

size of a hole leads to a different change in the fraction of the dielectric material. However, compared to waveguide-based designs, $\langle Q\rangle$ of *L*4/3 is only about 40% lower, while the mode volume is four times lower. In terms of the mode volume, the only 2D PhC cavity that can compete with *L*4/3 is the *H*0 cavity, with a V_m of $0.25(\lambda/n)^3$ and the highest experimentally demonstrated Q of 400 000.[27] However, the highest theoretical Q obtained for this value of V_m is one million,[34] while a further increase in the theoretical Q to 8.9 million is possible only at the expense of a mode-volume increase to $V_m = 0.64(\lambda/n)^3$. Moreover, despite its small volume, *H*0 has not found broad popularity due to the symmetry of its fundamental mode, which has a node in the center and electric field maxima at the interfaces of the two holes on each side. Furthermore, this symmetry results in an anti-node in the vertical direction of the far-field, which is a problem for applications in which light needs to be coupled in and out of the chip.[37]

There are two observations worth making as to why the inclusion of the extra air-holes leads to a significant decrease in the mode volume. The first one is the fact that from the perspective of the electromagnetic variational theorem, the energy functional is minimized when the electric field is inside the high-index material.[38] For the lowest-frequency localized mode, then, reducing the fraction of the dielectric content in the central region of the cavity decreases the physical space in which the electric field is preferentially confined, and the mode volume decreases. The same effect can be seen in other cavities with a decreased dielectric fraction.[8,39] Our low-V cavity mode is also related to the recently introduced "anti-slot" concept,[40–42] in which the electric field of polarization parallel to a silicon-air interface is strongly enhanced in a thin silicon slot. In the *L*4/3 cavity, this is exactly the situation in the $y = 0$ plane, in which the electric field polarization is in the y-direction, i.e., tangential to the air-hole interfaces. The connection to the anti-slot effect is especially clear in Fig. 2(b). However, outside of this plane, the electric field is generally not restricted to being tangential to the holes and is rather confined to the dielectric region because of the variational principle mentioned earlier. Furthermore, it is worth noting that we started from a low-V cavity design and *only* optimized the quality factor Q. In the future, the mode volume could be decreased further—albeit at the expense of the quality factor—by utilizing an objective function that takes both quantities into account.

Finally, we also demonstrate how efficient extraction of light can be achieved in the *L*4/3 cavity, using the paradigm in Refs. 43 and 44. The far field of the optimized design [Fig. 3(c)] has two peaks at very large angles, which makes free-space coupling of light in and out of the cavity very challenging. This is a typical feature of high-Q cavities but can be greatly improved by adding an *extractor* structure to the geometry. One possible realization of this is illustrated in Fig. 3(a), where the radius of the holes marked in red is increased from r to $r + r_e$. This modification has a periodicity twice larger than that of the PhC lattice and serves to fold Fourier components of the field that are normally outside of the light cone back into it. In this way, with only a small change in the radius, the extraction efficiency can be greatly improved, with the quality factor still remaining in the millions – as illustrated in Fig. 3(b). The efficiency η within a given collection angle θ_c around the normal direction is defined as

$$\eta(\theta_c) = \frac{\int_{\Omega(\theta_c)} |\mathbf{E}_{FF}(\theta,\phi)|^2 \sin(\theta)\mathrm{d}\theta\mathrm{d}\phi}{\int_{\Omega(90^\circ)} |\mathbf{E}_{FF}(\theta,\phi)|^2 \sin(\theta)\mathrm{d}\theta\mathrm{d}\phi}, \tag{2}$$

where $\Omega(\theta)$ is the solid angle from 0 to θ and $\mathbf{E}_{FF}$ are the far-field components of the electric field, computed through a near-to-far-field projection. In Fig. 3(b), we plot this efficiency for a collection angle of 30° [numerical aperture (NA) 0.5] as well as for 60° (NA = 0.87). The efficiency has a maximum for $r_e = 1$ nm and reaches a value of 0.65 in the first case and 0.93 in the second case. The far-field electric field profile for this value of r_e is shown in Fig. 3(d) and as expected presents a lobe centered around the vertical direction. Importantly, the quality factor remains very high,

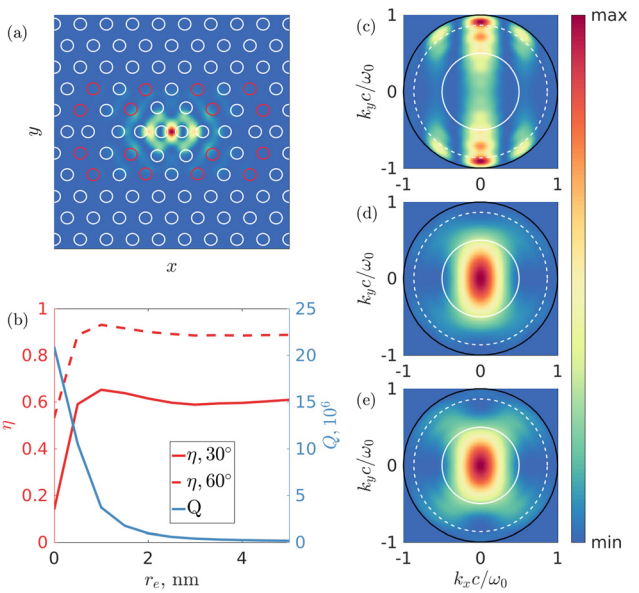

FIG. 3. (a) Optimized cavity design. For efficient vertical extraction, the radius of the holes marked in red is increased by r_e. (b) Extraction efficiency η and quality factor Q vs. the extractor radius r_e. (c)–(e) Normalized far-field intensity $|\mathbf{E}_{FF}|^2$ for the nominal design ($r_e = 0$ nm) (c), for $r_e = 1$ nm (d), and for $r_e = 3$ nm (e). The white solid line indicates a collection angle $\theta_c = 30^\circ$ from the vertical direction, while the dashed line $-\theta_c = 60^\circ$.

$Q = 3.7 \times 10^6$, and the mode volume does not change. Thus, a strong improvement in the coupling can be achieved without a significant compromise on the light confinement. Beyond $r_e = 1$ nm, the efficiency fluctuates only a little, but Q gets progressively lower as the overall strength of the radiative components increases. For completeness, we have also plotted the far-field profile for $r_e = 3$ nm in Fig. 3(e).

In conclusion, we have presented an ultra-high-Q photonic crystal slab cavity with a mode volume that is three times smaller than that of the optimized $L3$ design and four times smaller than that of waveguide-based cavities (see Table I). The mode profile of our structure presents a strong lobe in the center, making it ideal for coupling to quantum dots[11] or other optically active emitters.[45–48] We note that the positioning precision of the point-like source for such applications is the same as that needed for coupling to the $L3$ mode (see Fig. 1), i.e., in our cavity, the coupling strength can be significantly enhanced at no cost. This is also important when comparing with the nanobeam cavities based on the anti-slot effect,[40,41] which have a theoretical mode volume that is much smaller than $(\lambda/n)^3$, but would require extreme positioning precision for coupling to a point-like source. The $L4/3$ cavity is also relevant for enhancing the material non-linearity and can find applications for example for single-photon Kerr-effect blockades[49] or for unconventional photon blockades.[50] The possibility for efficient light extraction with a small compromise on the quality factor is an additional advantage for applications in both classical and non-classical light generation. Finally, we also note that the idea of introducing a defect in the photonic crystal lattice by *increasing* the number of holes (or, more generally, by decreasing the dielectric fraction) can be utilized to devise other cavities, as well as waveguides, with a stronger field confinement for smaller and more efficient devices.

This work was supported by the Swiss National Science Foundation through Project No. P2ELP2_165174.

[1]D. A. Miller, J. Lightwave Technol. **35**, 346 (2017).
[2]M. Notomi, Rep. Prog. Phys. **73**, 096501 (2010).
[3]Y. Akahane, T. Asano, B. Song, and S. Noda, Nature **425**, 944 (2003).
[4]Z. Zhang and M. Qiu, Opt. Express **12**, 3988 (2004).
[5]B. Song, S. Noda, T. Asano, and Y. Akahane, Nat. Mater. **4**, 207 (2005).
[6]E. Kuramochi, M. Notomi, S. Mitsugi, A. Shinya, T. Tanabe, and T. Watanabe, Appl. Phys. Lett. **88**, 041112 (2006).
[7]M. Notomi and H. Taniyama, Opt. Express **16**, 18657 (2008).
[8]A. Simbula, M. Schatzl, L. Zagaglia, F. Alpeggiani, L. C. Andreani, F. Schäffler, T. Fromherz, M. Galli, and D. Gerace, APL Photonics **2**, 056102 (2017).
[9]T. Asano, Y. Ochi, Y. Takahashi, K. Kishimoto, and S. Noda, Opt. Express **25**, 1769 (2017).
[10]Y. Lai, S. Pirotta, G. Urbinati, D. Gerace, M. Minkov, V. Savona, A. Badolato, and M. Galli, Appl. Phys. Lett. **104**, 241101 (2014).
[11]T. Yoshie, A. Scherer, J. Hendrickson, G. Khitrova, H. M. Gibbs, G. Rupper, C. Ell, O. B. Shchekin, and D. G. Deppe, Nature **432**, 200 (2004).
[12]D. Englund, D. Fattal, E. Waks, G. Solomon, B. Zhang, T. Nakaoka, Y. Arakawa, Y. Yamamoto, and J. Vučković, Phys. Rev. Lett. **95**, 013904 (2005).
[13]A. Faraon, I. Fushman, D. Englund, N. Stoltz, P. Petroff, and J. Vučković, Nat. Phys. **4**, 859 (2008).
[14]K. Rivoire, Z. Lin, F. Hatami, W. T. Masselink, and J. Vučković, Opt. Express **17**, 22609 (2009).
[15]S. Noda, M. Fujita, and T. Asano, Nat. Photonics **1**, 449 (2007).
[16]T. Yamamoto, M. Notomi, H. Taniyama, E. Kuramochi, Y. Yoshikawa, Y. Torii, and T. Kuga, Opt. Express **16**, 13809 (2008).
[17]C. Husko, A. D. Rossi, S. Combrie, Q. V. Tran, F. Raineri, and C. W. Wong, Appl. Phys. Lett. **94**, 021111 (2009).
[18]M. Nomura, N. Kumagai, S. Iwamoto, Y. Ota, and Y. Arakawa, Nat. Phys. **6**, 279 (2010).
[19]K. Nozaki, T. Tanabe, A. Shinya, S. Matsuo, T. Sato, H. Taniyama, and M. Notomi, Nat. Photonics **4**, 477 (2010).
[20]K. Nozaki, A. Shinya, S. Matsuo, Y. Suzaki, T. Segawa, T. Sato, Y. Kawaguchi, R. Takahashi, and M. Notomi, Nat. Photonics **6**, 248 (2012).
[21]B. Ellis, M. A. Mayer, G. Shambat, T. Sarmiento, J. Harris, E. E. Haller, and J. Vučković, Nat. Photonics **5**, 297 (2011).
[22]A. Reinhard, T. Volz, M. Winger, A. Badolato, K. J. Hennessy, E. L. Hu, and A. Imamoglu, Nat. Photonics **6**, 93 (2012).
[23]Y. Sato, Y. Tanaka, J. Upham, Y. Takahashi, T. Asano, and S. Noda, Nat. Photonics **6**, 56 (2012).
[24]T. Volz, A. Reinhard, M. Winger, A. Badolato, K. J. Hennessy, E. L. Hu, and A. Imamoglu, Nat. Photonics **6**, 605 (2012).
[25]A. Shakoor, R. Lo Savio, P. Cardile, S. L. Portalupi, D. Gerace, K. Welna, S. Boninelli, G. Franzò, F. Priolo, T. F. Krauss, M. Galli, and L. O'Faolain, Laser Photonics Rev. **7**, 114 (2013).
[26]Y. Takahashi, Y. Inui, M. Chihara, T. Asano, R. Terawaki, and S. Noda, Nature **498**, 470 (2013).
[27]U. P. Dharanipathy, M. Minkov, M. Tonin, V. Savona, and R. Houdré, Appl. Phys. Lett. **105**, 101101 (2014).
[28]A. Di Falco, L. O'Faolain, and T. F. Krauss, Appl. Phys. Lett. **94**, 063503 (2009).
[29]H. Hagino, Y. Takahashi, Y. Tanaka, T. Asano, and S. Noda, Phys. Rev. B **79**, 085112 (2009).
[30]M. Minkov, U. P. Dharanipathy, R. Houdré, and V. Savona, Opt. Express **21**, 28233 (2013).
[31]P. Barclay, K. Srinivasan, and O. Painter, Opt. Express **13**, 801 (2005).
[32]See http://www.lumerical.com/tcad-products/fdtd/ for Lumerical Solutions.
[33]Y. Akahane, T. Asano, B.-S. Song, and S. Noda, Opt. Express **13**, 1202 (2005).
[34]M. Minkov and V. Savona, Sci. Rep. **4**, 5124 (2014).
[35]MATLAB and Global Optimization Toolbox Release 2016b. The MathWorks, Inc., Natick, MA; available at http://www.walkingrandomly.com/?p=4767.
[36]L. C. Andreani and D. Gerace, Phys. Rev. B **73**, 235114 (2006).
[37]M. S. Mohamed, A. Simbula, J.-F. Carlin, M. Minkov, D. Gerace, V. Savona, N. Grandjean, M. Galli, and R. Houdré, APL Photonics **2**, 031301 (2017).
[38]J. D. Joannopoulos, S. G. Johnson, J. N. Winn, and R. D. Meade, *Photonic Crystals: Molding the Flow of Light* (Princeton University Press, 2008), Chap. 2.
[39]T. Asano, M. Mochizuki, S. Noda, M. Okano, and M. Imada, J. Lightwave Technol. **21**, 1370 (2003).
[40]S. Hu and S. M. Weiss, ACS Photonics **3**, 1647 (2016).
[41]H. Choi, M. Heuck, and D. Englund, Phys. Rev. Lett. **118**, 223605 (2017).
[42]S. Hu, M. Khater, R. Salas-Montiel, E. Kratschmer, S. Engelmann, W. M. J. Green, and S. M. Weiss, preprint arXiv:1707.04672 (2017).
[43]N.-V.-Q. Tran, S. Combrié, and A. De Rossi, Phys. Rev. B **79**, 041101 (2009).
[44]S. L. Portalupi, M. Galli, C. Reardon, T. Krauss, L. O'Faolain, L. C. Andreani, and D. Gerace, Opt. Express **18**, 16064 (2010).
[45]A. Faraon, C. Santori, Z. Huang, V. M. Acosta, and R. G. Beausoleil, Phys. Rev. Lett. **109**, 033604 (2012).
[46]B. J. M. Hausmann, B. J. Shields, Q. Quan, Y. Chu, N. P. De Leon, R. Evans, M. J. Burek, A. S. Zibrov, M. Markham, D. J. Twitchen, H. Park, M. D. Lukin, and M. Loncăr, Nano Lett. **13**, 5791 (2013).
[47]G. Calusine, A. Politi, and D. D. Awschalom, Appl. Phys. Lett. **105**, 011123 (2014).
[48]A. Sipahigil, R. E. Evans, D. D. Sukachev, M. J. Burek, J. Borregaard, M. K. Bhaskar, C. T. Nguyen, J. L. Pacheco, H. A. Atikian, C. Meuwly, R. M. Camacho, F. Jelezko, E. Bielejec, H. Park, M. Lončar, and M. D. Lukin, Science **354**, 847 (2016).
[49]S. Ferretti and D. Gerace, Phys. Rev. B **85**, 33303 (2012).
[50]H. Flayac, D. Gerace, and V. Savona, Sci. Rep. **5**, 11223 (2015).